Video Article

Multi-material Ceramic-Based Components – Additive Manufacturing of Black-and-white Zirconia Components by Thermoplastic 3D-Printing (CerAM - T3DP)

Steven Weingarten[1], Uwe Scheithauer[1], Robert Johne[2], Johannes Abel[1], Eric Schwarzer[1], Tassilo Moritz[1], Alexander Michaelis[1]

[1]Fraunhofer Institute for Ceramic Technologies and Systems IKTS

[2]Fraunhofer Singapore

Correspondence to: Steven Weingarten at steven.weingarten@ikts.fraunhofer.de

Abstract

To combine the benefits of Additive Manufacturing (AM) with the benefits of Functionally Graded Materials (FGM) to ceramic-based 4D components (three dimensions for the geometry and one degree of freedom concerning the material properties at each position) the Thermoplastic 3D-Printing (CerAM - T3DP) was developed. It is a direct AM technology which allows the AM of multi-material components. To demonstrate the advantages of this technology black-and-white zirconia components were additively manufactured and co-sintered defect-free.

Two different pairs of black and white zirconia powders were used to prepare different thermoplastic suspensions. Appropriate dispensing parameters were investigated to manufacture single-material test components and adjusted for the additive manufacturing of multi-color zirconia components.

Video Link

The video component of this article can be found at https://www.jove.com/video/57538/

Introduction

Functionally Graded Materials (FGM) are materials with a variety of properties concerning transitions in the microstructure or in the material[1]. These transitions can be discrete or continuous. Different kinds of FGM are known, such as components with material gradients, graded porosity as well as multi-colored components.

FGM-components can be manufactured by single conventional shaping technologies[2,3,4,5,6,7] or by a combination of these technologies, for example, by in-mold labeling as a combination of tape casting and injection molding[8,9].

Additive manufacturing (AM) allows for the production of components with a so far unprecedented freedom of design. This is considered the state of the art shaping technology for polymers and metals. First commercial processes for the processing of ceramics are available[10], and nearly all known AM technologies are used for AM of ceramics in laboratories all over the world[11,12,13].

To combine the benefits of AM with the benefits of FGM to ceramic-based 4D components (three dimensions for the geometry and one degree of freedom concerning the material properties at each position) the Thermoplastic 3D-Printing (CerAM - T3DP) has been developed at Fraunhofer IKTS in Dresden, Germany, as a direct AM technology. This allows the AM of multi-material components[14,15,16,17]. CerAM - T3DP is based on the selective deposition of single droplets of particle filled thermoplastic suspensions. By utilizing multiple dosing systems, different thermoplastic suspensions can be deposited beside each other layer by layer to produce bulk material as well as property gradients within the additively manufactured green components[18]. Unlike indirect AM processes, in which previously deposited materials solidify selectively over the entire layer, the CerAM - T3DP process does not require the additional effort of removing any non-solidified material prior to the deposition of the next material, making it more suitable for the AM of multi-material components.

Although utilizing the CerAM - T3DP process allows the AM of FGM and the realization of ceramic-based components with unprecedented properties, there are challenges to overcome regarding the necessary thermal treatment after the AM process, in order to obtain a multi-material composite. In particular, the paired powders in the composite material need to be successfully co-sintered, for which the sintering of the components has to be performed at the same temperature and atmosphere. Therefore, it is a prerequisite for all materials to have a comparable sintering temperature and behavior (starting temperature of sintering, shrinkage behavior). In order to avoid critical mechanical stress during cooling, the coefficient of thermal expansion of all materials has to be approximately equal[11].

The combination of materials with different properties in one component opens the door to components with unprecedented properties for manifold applications. *E.g.* stainless steel-zirconia composites can be used as cutting tools, wear resistant components, energy, and fuel cell

components or as bipolar surgical tools[19,20,21,22,23,24]. Such components could be realized by CerAM - T3DP[14,15,16,17], too, after the adjustment of the sintering behavior by a special milling process[16].

Ceramic-based FGM with a graded porosity like dense and porous zirconia combine very good mechanical properties in the dense areas with a high active surface of the porous areas. Such like components can be additively manufactured by CerAM - T3DP[18].

In this paper, we investigate the AM of zirconia components with two different colors in one component by CerAM - T3DP. We chose white and black zirconia because this combination in one ceramic component is interesting for jewelry applications. The demand of individualized luxury goods is very high and still growing. Technologies which allow the AM of ceramic-based multi-material components with a high resolution and very good surface properties will allow to satisfy this demand. Ceramics like zirconia are used for example to produce watch components like watch cases and bezels or for rings because of the special haptics, glance, hardness and lower weight compared to metals.

Protocol

1. Thermoplastic Suspension for CerAM - T3DP

1. Selection of powders
    1. For the preparation of the black thermoplastic suspensions use black zirconia powders *zirconia black - 1* and *zirconia black - 2*.
    2. For the preparation of the white thermoplastic suspensions use *zirconia white - 1* and *zirconia white - 2*.
    NOTE: The manufacturer of *zirconia black - 2* uses pigments (4.2 wt.-%) for the coloring of the zirconia and also states that both powders have the same sintering behavior. Additionally, the high percentage of alumina (20.43 wt.-%) contributes to the white color of *zirconia white - 2*. The powders *zirconia black - 1* and *zirconia white - 1* have a different composition and thus require a different sintering temperature for complete densification. In contrast to *zirconia white - 1*, *zirconia black - 1* consists at most 5 wt.-% pigments. The recommended sintering temperatures are 1400 °C for *zirconia black - 1* and 1350 °C for *zirconia white - 1*.
2. Characterize the powders regarding shape, surface area and particle size distribution.
   NOTE: Electron scanning microscopy images have been used to characterize the shape of the particles. The particle size distribution of the utilized powders was measured by a laser diffraction method (*laser diffractometer*). The measurements for the specific surface properties of the used powders have been provided by the manufacture.
3. For the preparation of the different zirconia suspensions melt a mixture of paraffin and beeswax at a temperature of 100 °C in a heatable *dissolver* and homogenize the polymer mixture.
    1. Then add the powder in several steps to reach a powder content of 40 vol.%.
    2. Homogenize the powder-polymer-mixture by stirring for 2 h at 100 °C. Ensure that all suspensions have the same powder content (40 vol.%).
4. Characterization of suspensions
    1. Characterize the rheological behavior of the molten suspension using a *rheometer* for shear rates in a range between 0-5,000/s for different temperatures in a range between 85 °C and 110 °C.
    NOTE: We used a *rheometer* adjustable between -25 °C to 200 °C with a plate/plate measuring system (25 mm diameter). The torque was measured, and the dynamic viscosity was calculated.
    2. Plot the dynamic viscosity as function of the shear rate and make sure that the dynamic viscosity is below 100 Pa·s for a shear rate of 10/s, below 20 Pa·s for a shear rate of 100/s and below 1 Pa·s for a shear rate of 5,000/s or increase the temperature within the permissible range.
    3. Change the suspension composition by adding polymer mixture if the dynamic viscosity is too high even for a temperature of 110 °C.

2. Manufacturing of Single and Multi-Material Components by CerAM - T3DP

1. Used device
   Figure 1 shows a CAD-drawing of the used CerAM - *T3DP-device* with one *profile scanner* and three different *micro dispensing systems*, which can work simultaneously or alternately. Use two of them to produce black-and-white components.
    1. Set the deposition of the droplets to a frequency up to 100/s and the axes to move with a maximum velocity of 20 mm/s.
2. Investigation of deposition parameters
   Investigate the influence of deposition parameters (working velocities of the micro dispensing system; temperatures of suspension reservoir and nozzle; velocity of the axis) on the properties of the resulting droplets (shape; volume; homogeneity) or droplet chains (shape; volume; homogeneity).
    1. Vary the deposition parameters and deposit single droplets as well as droplet chains by using different frequencies and axes velocities for deposition.
    NOTE: The influence of the dispenser parameters on the properties of the materials has been discussed before[25]. Parameter value boundaries have only been determined empirically.
    2. Make sure that that the variance in droplet chain height and width should not exceed 3 %. Vary the parameters pulse width, droplet fusion factor (DFF) and extrusion width (slicing parameter) to compensate diameter differences up to 100 microns and height differences up to 50 microns.
    NOTE: It is not necessary and probably not possible to realize perfectly shaped hemispheres as single droplets, but you have to make sure that the homogeneity of the droplet formation is very high to guarantee a homogenous building of the components.
    3. Repeat this step with different initial parameters to find a parameter set which provides the most homogenous droplet shape with respect to droplet diameter, width and height.

3. Manufacturing of single-material test components
   1. Use a generated 3D model of the desired part and save the file as STL or AMF file format.
   2. Use a slicing program (e.g. *Slicer 1* or *Slicer 2*) to generate the corresponding G-code. Set the properties for the droplet shape acquired in step 2.2.
   3. Upload the G-code and fill the process parameters to the CerAM - T3DP-device. Set the CerAM - T3DP-device for the parameters obtained in step 2.2 that did correspond to the droplet shape provided to the slicer. Start the device software to start the building job.
   NOTE: It is beneficial to manufacture certain test samples before building the desired part or using new suspensions.

4. CerAM - T3DP of multi-material components
   1. For each material involved execute step 2.2.
   2. Select dispensing parameters for both materials which have approximately the same droplet characteristics.
   3. Adjust the layer heights by changing the distance between the single droplets and the resulting overlap to avoid differences in heights for the different materials, which can result in large defects and faulty components.
   NOTE: By reducing the distance between two droplets and the associated greater overlap, the width and height of the droplet chain increases due to the nearly constant volume of the single droplets. It can be observed that the droplet chain width increases faster than the droplet chain height.
   4. Use a generated 3D model of the desired part and save the file as AMF files. If supported by the slicer multiple component areas can also be saved in STL file format.
   5. In order to print multi-material components, assign corresponding component areas to the associated material in the slicing software by allocating a corresponding *micro dispensing system* for each material.
   6. Generate the G-codes for each material by using the slicer software.
   7. Upload the G-code and fill the process parameters to the CerAM - T3DP-device. Set the CerAM - T3DP-device for the parameters obtained in step 2.2 that did correspond to the droplet shape provided to the slicer. Start the device software to start the building job.

3. Co-Debinding and Co-Sintering of Single- and Multi-Material Components

1. Debind the green samples in the following separate steps.
   1. First, put the samples in a loose bulk of coarse-grained alumina powder (powder bed) to structurally support the samples as well as to ensure a homogeneous temperature distribution and to promote the removal of the binder materials by capillary forces.
   2. Perform a debinding with a very low heating rate in a furnace (*debinding furnace*) under air-atmosphere up to 270 °C. Set the heating rate to 4 K/h to ensure a defect-free debinding.

2. After this first debinding step carefully remove the bedding powder for example with a fine brush. Place the samples on alumina kiln furniture.
3. Apply a second debinding step under air-atmosphere up to 900 °C (12 K/h) in the same furnace.
   NOTE: All remaining organic binder materials were thermally removed, while within in the same step a pre-sintering of the zirconia particles was initiated to enable the subsequent transfer of the samples to a sintering kiln.
4. Finally sinter the samples under air-atmosphere at 1,350 °C (180 K/h) for 2 h in a suitable furnace (*sintering furnace*). Characterize the shrinkage of the components by length measurement in three dimensions and make sure that it is about 20% for each direction.

4. Characterization of Single- and Multi-Material Components

1. Cut the samples properly and polish the surface using ceramographic methods.
2. Apply investigations on the microstructure by using Field Emission Scanning Electron Microscope (*FESEM*).
3. Visually inspect the porosity of the two phases and at the boundary interface of the used materials. To obtain a more detailed result perform an interface analysis, e.g. by *FESEM* and subsequent picture analysis to investigate the porosity within the sintered microstructure.
   The targeted porosity is below 1%. If the porosity is too high, vary the deposition parameter rising (2.2) and/or the regime of the thermal treatment (3).

Representative Results

For the production of measured components, only powders of the same manufacturer have been combined for each multi-material component. Experiments with powders of different manufactures in one component are still ongoing. For this purpose, the different shrink rates have to be considered.

The measurement result of the average particle diameter (d50) of the *zirconia white - 1* after dispersion was 0.37 µm. The manufacturer states an actual particle size of 0.04 µm (one order of magnitude less). The average particle size (d50) of the *zirconia black - 1* is 0.5 µm. **Figure 2 (A)** shows the FESEM analysis of the *zirconia white - 1* and **Figure 2 (B)** a FESEM-image of the surface of a granulate in detail. **Figure 2 (C)** and **Figure 2 (D)** show the same for *zirconia black - 1*. Both untreated powders consist of big spherical granules (diameter up to 100 µm) which is typical for dry pressing raw materials. The FESEM-images of the granulate surfaces show the primary particles of the *zirconia white - 1* (**Figure 2 (B)**) and *zirconia black - 1* (**Figure 2 (D)**) with an actual particle size of almost 0.04 µm.

The **Figure 2 (E)** – **2 (H)** show the FESEM-images of the *zirconia white - 2* and *zirconia black - 2*. The measured average particle sizes (d50) of the zirconia powders *zirconia white - 2* and *zirconia black - 2* are 0.27 µm and 0.25 µm, respectively, wherein the particles are present as spherical granules with diameters up to 100 µm (**Figure 2 (E)** and **Figure 2 (G)**). The size of the white powders primary particles is below 0.1 µm (**Figure 2 (F)**). The black powders primary particles are up to 0.5 µm in diameter (**Figure 2 (H)**).

Figure 3 (A) shows the dynamic viscosity of the suspensions based on *zirconia white - 1* and *zirconia black - 1* as a function of the shear rate and in dependence of the temperature (85 °C and 100 °C). Both suspensions show a shear thinning behavior regardless of the temperature.

Table 1 summarizes the measured viscosities of the suspensions at different shear rates and for different temperatures.

Figure 3 (B) shows the rheological behavior of the suspensions based on *zirconia white - 2* and *zirconia black - 2* (85 °C and 100 °C). All graphs show a shear thinning behavior. **Table 2** summarizes the measured viscosities of the suspensions at different shear rates and for different temperatures.

In addition to shear rate-controlled measurements, long-term measurements were carried out. **Figure 3 (C)** shows the course of the dynamic viscosity during the long-term measurements for all four suspensions at a constant shear rate of 10/s over 2 h. While the dynamic viscosity of the white zirconia suspensions (*zirconia white - 1* and *zirconia white - 2*) is nearly constant (**Table 3**), the dynamic viscosity tends to decrease slightly of the black zirconia (*zirconia black - 1* and *zirconia black - 2*).

After the empirical determination of the dosing parameters the manufacturing of single component, three dimensional structures became manageable for each suspension. **Figure 4 (A)** shows a complex sintered test structure based on the suspension made of *zirconia white - 1 and* additively manufactured by CerAM - T3DP. The same test structure additively manufactured by CerAM - T3DP and the *zirconia black - 1*-suspension is shown in **Figure 4 (B)**.

Figure 4 (C) shows a sintered test structure based on the zirconia suspensions of the *zirconia white - 2*, **Figure 4 (D)** a sintered test structure based on *zirconia black - 2*. Subsequent to the manufacturing of the single-color components the manufacturing of multi-color components took place. The **Figure 4 (D)** to **4 (F)** show some sintered multi-color zirconia components additive manufacturing using the CerAM - T3DP.

Figure 5 (A) and **Figure 5 (B)** show FESEM-images of the microstructure of multi-color components with a clearly distinguishable interface between the two suspensions based on the zirconia powders *zirconia white - 1* (top) and *zirconia black - 1* (bottom).

An energy-dispersive X-ray spectroscopic analysis (EDX) showed that in the microstructure of the sintered *zirconia black - 1* more alumina crust occurs (**Figures 6 (A-C)**). To evaluate the composition of the and *zirconia black - 1*-microstructure especially in the dark areas in more detail further EDX investigations took place (**Figures 6 (D-G)**) which showed the precipitation of alumina (**Figure 6 (E)**).
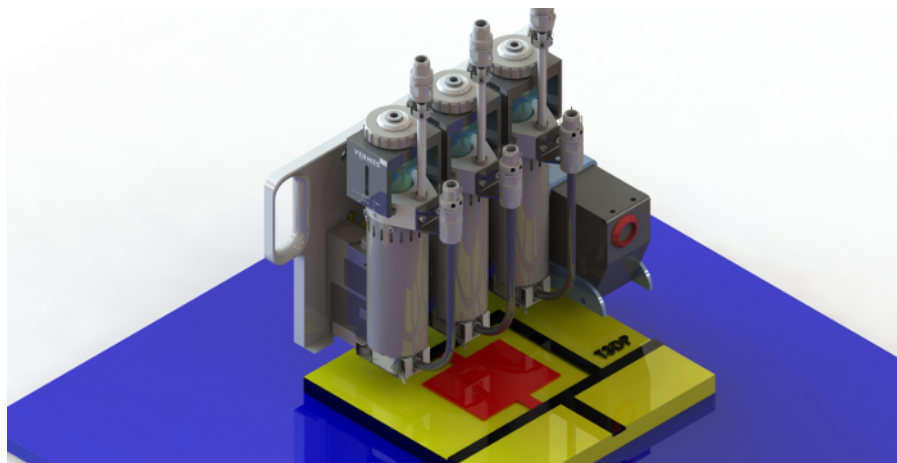

Figure 1: CAD-drawing of used CerAM - T3DP-device with three micro dispensing units and one surface scanner. Please click here to view a larger version of this figure.
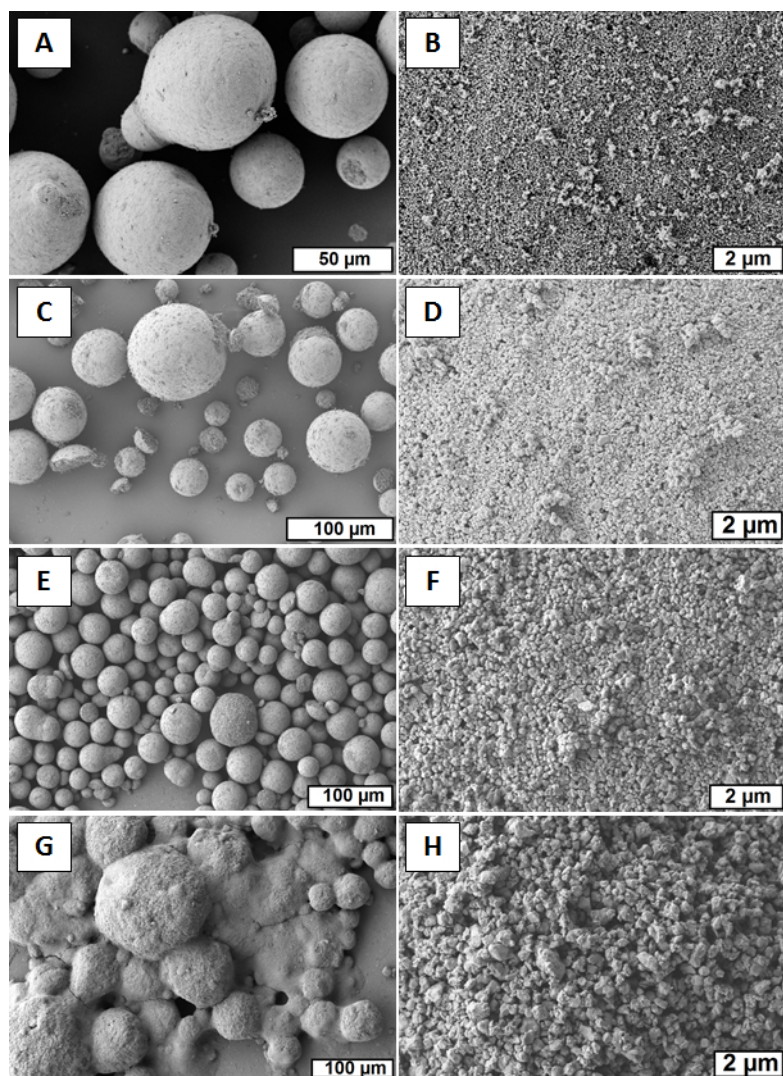
Figure 2: FESEM-image of used zirconia granulates. (A) *zirconia white - 1* granulates - overview and **(B)** surface; **(C)***zirconia black - 1* granulates - overview and **(D)** surface; **(E)** *zirconia white - 2* granulates - overview and **(F)** surface; **(G)** *zirconia black - 2* granulates - overview and **(H)** surface.
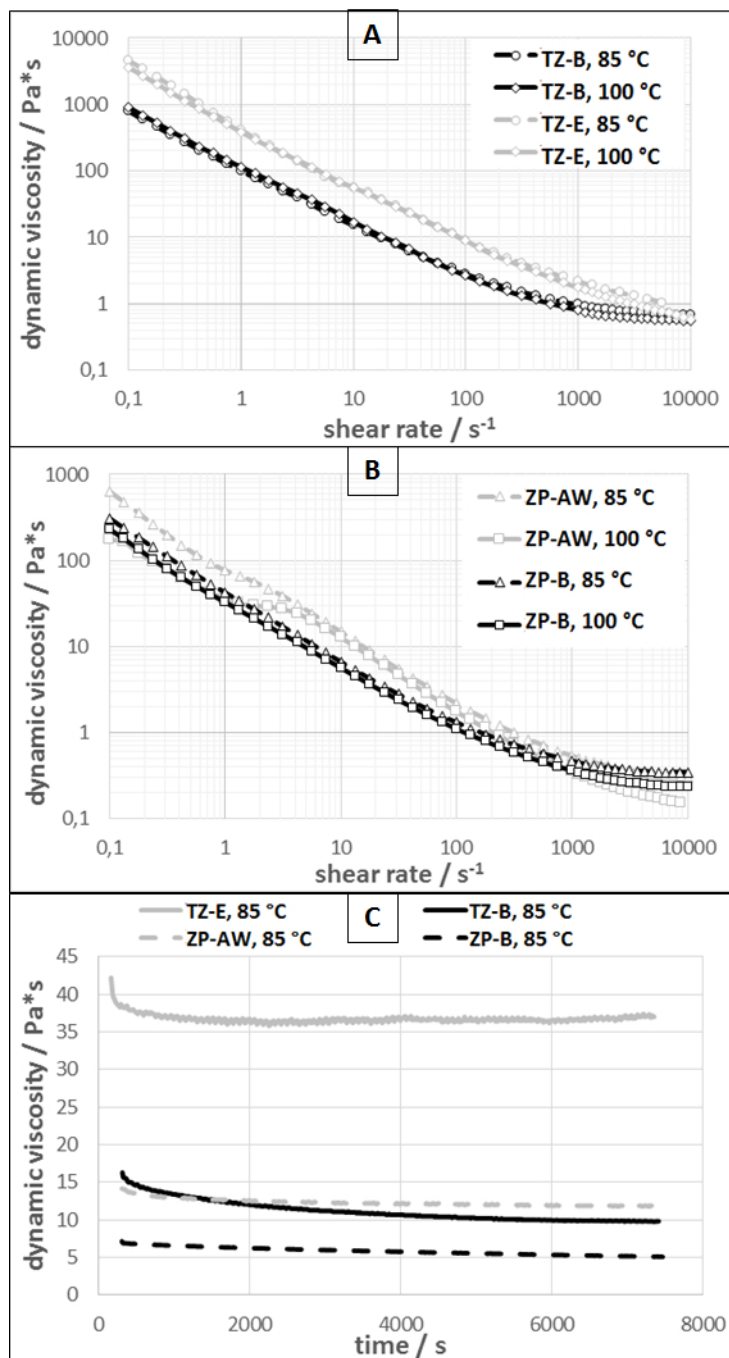
Figure 3: Rheological behavior of thermoplastic suspensions. (A) based on the zirconia powders *zirconia white - 1* and *zirconia black - 1*; **(B)** based on the zirconia powders *zirconia white - 2* and *zirconia black - 2*; **(C)** comparison of all four suspensions during a long-term measurement at a constant shear rate of 10/s.
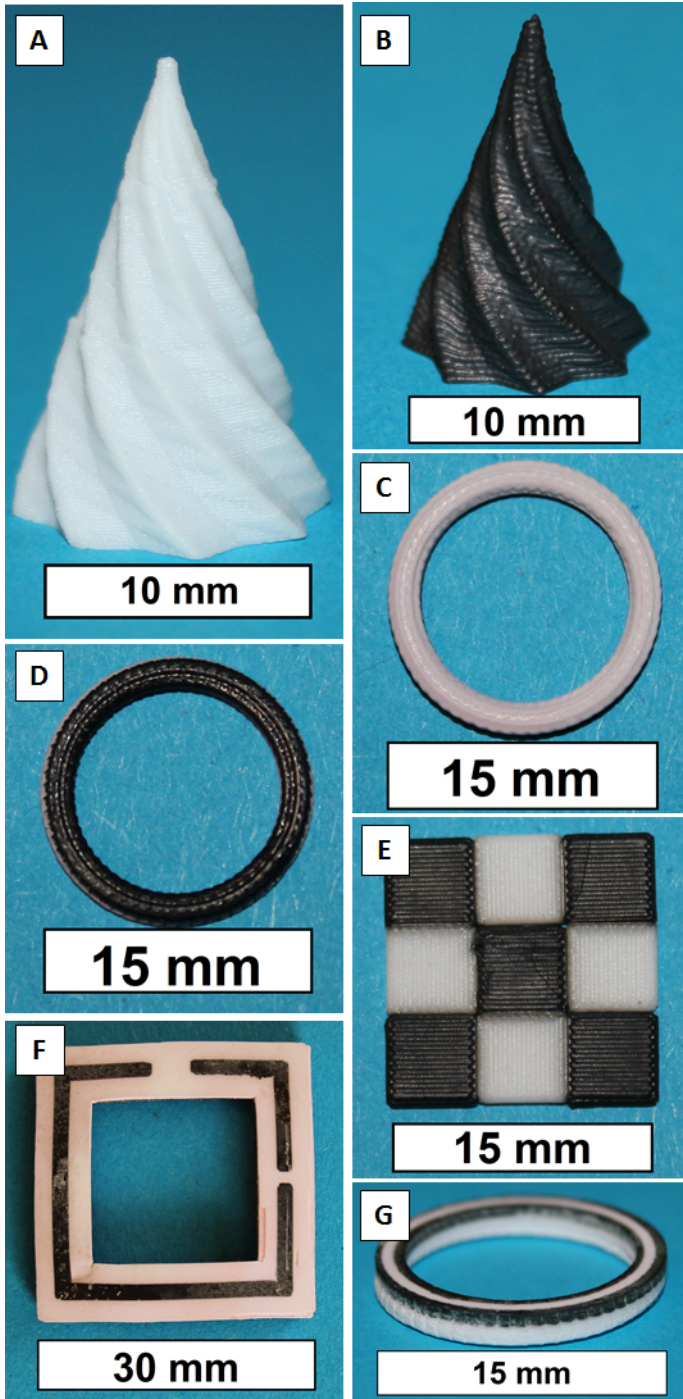
Figure 4: Sintered single- and multi-material test structures additively manufactured by T3DP. (A) based on *zirconia white - 1* -suspension; **(B)** based on *zirconia black - 1* -suspension; **(C)** based on *zirconia white - 2* -suspension; **(D)** based on *zirconia black - 2* -suspension; **(E)** based on *zirconia white - 1* - and *zirconia black - 1* -suspension; **(F)** based on *zirconia white - 2*- and *zirconia black - 2* -suspension - frame-like structure and **(G)** ring-like structure.
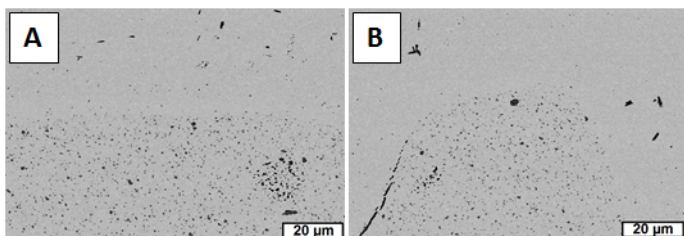
Figure 5: FESEM-images. FESEM-images of cross section at interface between sintered *zirconia white - 1* (top) and *zirconia black - 1* (bottom); **(A)** planar interface and **(B)** interwoven interface
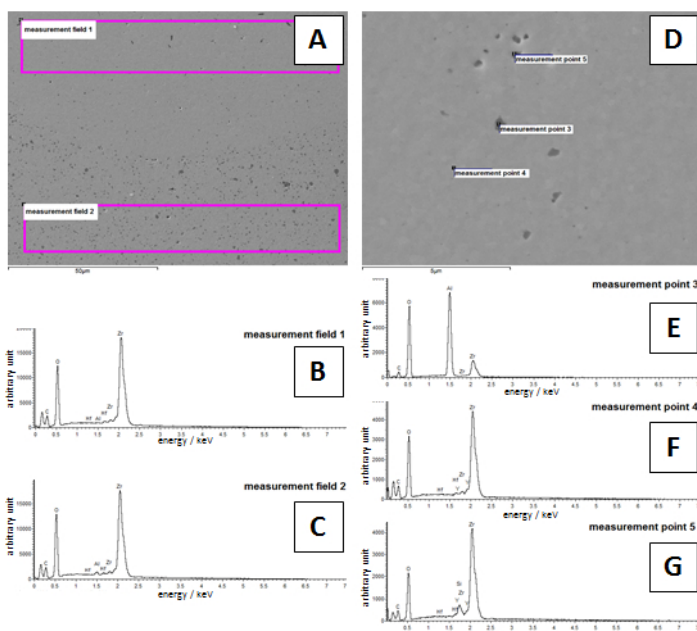

Figure 6: Results of EDX measurements at sintered *zirconia white - 1* / *zirconia black - 1* -interface. (A) Overview about measurement fields 1 + 2 and **(D)** 3 - 5; results of measurement **(B)** field 1, **(C)** field 2, **(E)** field 3, **(F)** field 4 and **(G)** field 5.
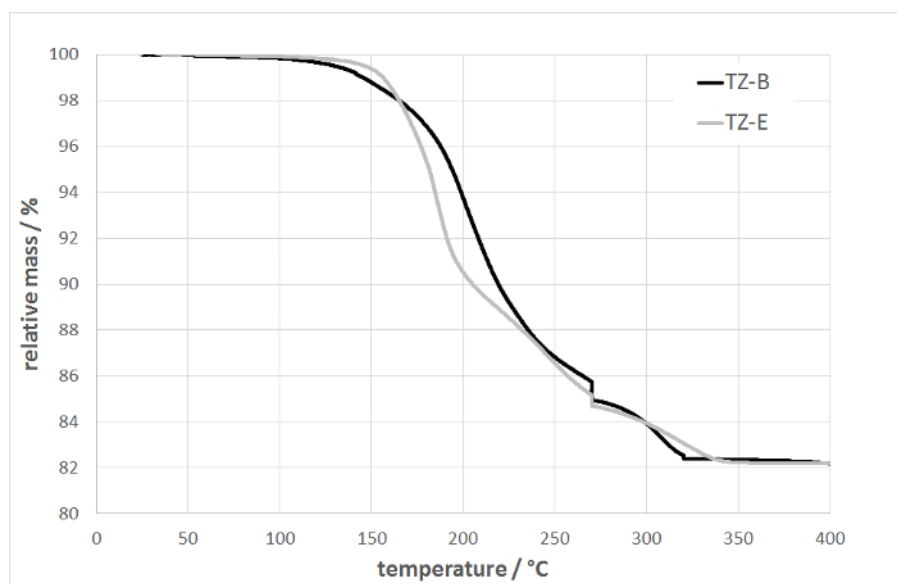

Figure 7: Mass change of the *zirconia white - 1-* and *zirconia black - 1* -suspensions during thermal decomposition Please click here to view a larger version of this figure.

used zirconia powder	temperature / °C	shear rate / s⁻¹					
		0.1	1	10	100	1000	10000
TZ-E	85	4600	414	56.60	8.98	2.16	0.59
	100	3630	386	56.00	8.96	1.75	0.57
TZ-B	85	791	99	15.20	2.82	0.97	0.67
	100	905	114	13.30	2.66	0.81	0.55

dynamic viscosity / Pa·s

Table 1: Dynamic viscosity of thermoplastic suspensions based on the zirconia powders *zirconia white - 1* and *zirconia black - 1*. Please click here to download this file.

used zirconia powder	temperature / °C	shear rate / s⁻¹					
		0.1	1	10	100	1000	10000
ZP-AW	85	637	76.50	14.8	2.19	0.54	0.30
	100	173	35.5	12.7	1.74	0.35	0.15
ZP-B	85	310	42.4	6.66	1.31	0.47	0.35
	100	231	32.7	5.64	1.1	0.36	0.23

dynamic viscosity / Pa·s

Table 2: Dynamic viscosity of thermoplastic suspensions based on the zirconia powders *zirconia white - 2* and *zirconia black - 2*. Please click here to download this file.

used zirconia powder	time / s						
	1000	2000	3000	4000	5000	6000	7000
TZ-E	36.8	36.7	36.8	36.7	36.8	36.6	36.8
TZ-B	13.4	12.0	11.2	10.7	10.2	9.95	9.84
ZP-AW	13.0	12.6	12.3	12.1	12.0	11.9	11.9
ZP-B	6.5	6.2	6.0	5.8	5.6	5.4	5.2

dynamic viscosity / Pa·s

Table 3: Dynamic viscosity of all four suspensions during the long-term measurement at a constant shear rate of 10/s. Please click here to download this file.

Discussion

The characterization of the rheological behavior of the molten suspension at high shear rates up to 5000/s is necessary since the assessment of the conditions within the used micro dispensing systems (geometry of piston and nozzle chamber, velocity of piston) revealed that shear rates of 5000/s and higher are generated in the micro dispensing system during the deposition process[25].

The investigation of the printing parameters should be done to aid with the calibration of the dispenser for the manufacturing of multi-material components. The influence of the dispenser parameters on the properties of the materials has been discussed in[25]. Parameter value boundaries have only been determent empirically. Experience so far shows that the variance in droplet chain height and width should not exceed 3 %. Diameter differences up to 100 microns and height differences up to 50 microns can be compensated by the parameters pulse width, droplet fusion factor (DFF) and extrusion width (slicing parameter).

It is critical for the printing process that the layer heights of the different materials are adjusted to each other by changing the distance between the single droplets, since it would result in an unevenness within a layer if the heights of the different materials do not match. An unevenness leads to large defects and faulty components. By reducing the distance between two droplets and the associated greater overlap, the width and height of the droplet chain increases due to the nearly constant volume of the single droplets. It can be observed that the droplet chain width increases faster than the droplet chain height.It is not necessary and probably not possible to realize perfectly shaped hemispheres as single droplets, but you have to make sure by determining the fitting dispensing parameters that the homogeneity of the droplet formation is very high to guarantee a homogenous building of the components.

The measurement at 85 °C simulates the rheological behavior of the suspensions in the feeding cartridge of the micro dispensing system. Above 90 °C, the decomposition of the binder components begins (**Figure 7**). All suspensions show nearly similar behavior. The used nozzle temperature of the micro dispensing system was 100 °C. This temperature promotes the droplet formation due to the low viscosity caused by increasing the suspensions temperature while passing the nozzle. Because of the short dwell time of the suspensions within the nozzle at this temperature the decomposition is not influencing the material behavior significantly.

The multi-color components could be sintered nearly defect-free, but for the *zirconia black - 2* and *zirconia white - 2* powders the color of the white phase turned into pink. The cause for the color change are diffusion processes between the different materials during sintering. This is only an effect at the surface and can be removed by a grinding step. But this is very challenging for complex structures made by AM technologies.

Within the multi-color components planar and interwoven boundary interfaces developed between the two different compositions. Thus, regardless of the drop-bound deposition of the material, the arrangement of the different microstructures can be realized very precisely.

Furthermore, the droplet shape can be exploited to increase the boundary interface between two materials. So far only discrete material transitions have been produced. Future research may also involve the production of gradual changes between materials.

Disclosures

The authors have nothing to disclose.

Acknowledgements

References

1. Kieback, B., Neubrand, A., Riedel, H. Processing techniques for functionally graded materials. *Materials Science and Engineering - A.* **362** (1-2), 81-106 (2003).
2. Mortensen, A., Suresh, S. Functionally graded metals and metal-ceramic composites: Part 1 Processing. *International Materials Reviews.* **40** (6), 239-265 (1995).
3. Moya, J.S., Sánchez-Herencia, A.J., Requena, J., Moreno, R. Functionally gradient ceramics by sequential slip casting. *Materials Letters.* **14** (5), 333-335 (1992).
4. Moya, J.S., Sánchez-Herencia, J.A., Bartolomé, J.F., Tanimoto, T. Elastic modulus in rigid Al2O3/ZrO2 ceramic laminates. *Scripta Materialia.* **37** (7), 1095-1103 (1997).
5. Zschippang, E., Mannschatz, A., Klemm, H., Moritz, T., Martin, H.-P. Charakterisierung und Verarbeitung von Si$_3$N$_4$-SiC-MoSi$_2$-Kompositen für Heizleiteranwendungen. *Keramische Zeitschrift.* **65** (5), 294-297, (2013).
6. Scheithauer, U., Haderk, K., Richter, H.-J., Petasch, U., Michaelis, A. Influence of the kind and amount of pore forming agents on the thermal shock behaviour of carbon-free refractory components produced by multilayer technology. *refractories WORLDFORUM.* **4** (1), 130-136, (2011).
7. Scheithauer, U., Schwarzer, E., Slawik, T., Richter, H.-J., Moritz, T., Michaelis, A. Functionally Graded Materials Made by Water-Based Multilayer Technology. *Refractories Worldforum.* **8** (2), 95 - 101, (2016).
8. Mannschatz, A., Härtel, A., Müller-Köhn, A., Moritz, T., Michaelis, A., Wilde, M. Manufacturing of Two-colored Co-sintered Zirconia Components by Inmold-labelling and 2C-Injection Molding, cfi/Ber. *DKG.* **91** (8), (2014).
9. Moritz, T., Scheithauer, U., Mannschatz, A., Ahlhelm, M., Abel, J., Schwarzer, E., Pohl, M., Müller-Köhn, A. Material- and process hybridization for multifunctional ceramic and glass components. *Ceramic Applications.* **5** (2), 66-71, (2017).
10. Homa, J. Rapid Prototyping of high-performance ceramics opens new opportunities for the CIM industry. *Powder Injection Moulding International.* **6** (3), 65-68, (2012).
11. Chartier, T., Badev, A. Rapid Prototyping of Ceramics. *Handbook of Advanced Ceramics Elsevier.* Oxford, UK, (2013).
12. Travitzky, N. *et al.* Additive Manufacturing of ceramic-based materials. *Advanced Engineering Materials.* **16**, 729-754 (2014).
13. Zocca, A., Colombo, P., Gomes, C. M., Günster, J. Additive Manufacturing of Ceramics: Issues, Potentialities, and Opportunities. *Journal of the American Ceramic Society.* **98** (7), 1983-2001 (2015).
14. Scheithauer, U., Schwarzer, E., Richter, H.J., Moritz, T. Thermoplastic 3D Printing - An Additive Manufacturing Method for Producing Dense Ceramics. *JACT.* **12** (1), 26-31 (2014).
15. Scheithauer, U., Bergner, A., Schwarzer, E., Richter, H.-J., Moritz, T. Studies on thermoplastic 3D printing of steel-zirconia composites. *J Mat Res.* **29** (17), 1931 - 1940 (2014).
16. Scheithauer, U., Slawik, T., Schwarzer, E., Richter, H.-J., Moritz, T., Michaelis, A. Additive Manufacturing of Metal-Ceramic-Composites by Thermoplastic 3D-Printing. *J. Ceram. Sci. Tech.* **06** (02), 125-132 (2015).
17. Scheithauer, U., Schwarzer, E., Haertel, A., Richter, H.J., Moritz, T.; Michaelis, A. Processing of thermoplastic suspensions for Additive Manufacturing of Ceramic- and Metal-Ceramic-Composites by Thermoplastic 3D-Printing (T3DP), 11th International Conference on Ceramic Materials and Components for Energy and Environmental Applications, *Ceramic Transactions.* **256** (2016).
18. Scheithauer, U., Weingarten, S., Johne, R., Schwarzer, E., Abel, J., Richter, H., Moritz, T., Michaelis, A. Ceramic-Based 4D-Components: Additive Manufacturing (AM) of Ceramic-Based Functionally Graded Materials (FGM) by Thermoplastic 3D-Printing (T3DP). *Preprints.* 2017100057 (2017).
19. Lee, H.C., Potapova, Y., Lee, D. A core-shell structured, metal-ceramic composite supported Ru catalyst for methane steam reforming. *J of Power Sources.* **216**, 256-260 (2012).
20. Molin, S., Tolczyk, M., Gazda, M., Jasinski, P. Stainless steel/yttria stabilized zirconia composite supported solid oxide fuel cell. *J. Fuel Cell Sci. Technol.* **8**, 1-5 (2011).
21. Roberts, H.W., Berzins, D.W., Moore, B.K., Charlton, D.G. Metal-Ceramic Alloys in Dentistry: A Review. *Journal of Prosthodontics.* **18** (2), 188-194 (2009).
22. Largiller, G., Bouvard, D., Carry, C.P., Gabriel, A., Müller, J., Staab, C. Deformation and cracking during sintering of bimaterial components processed from ceramic and metal powder mixes. Part I: Experimental investigation. *Mechanics of Materials.* **53**, 123-131 (2012).
23. Meulenberg, W. A., Mertens, J., Bram, M., Buchkremer, H.-P., Stöver, D. Graded porous TiO$_2$ membranes for micro-filtration. *Journal European Ceramic Society.* **26**, 449-454 (2006).
24. Baumann, A., Moritz, T., Lenk, R. Multi component powder injection moulding of metal-ceramic-composites. *Proceedings of the Euro International Powder Metallurgy Congress and Exhibition.* (2009).
25. Scheithauer, U., Johne, R., Weingarten, S., Schwarzer, E., Abel, J., Richter, H., Moritz, T., Michaelis, A. Investigation of Droplet Deposition for Suspensions Usable for Thermoplastic 3D Printing (T3DP). *Journal of Materials Engineering and Performance.* (2017).